

Electrochemical and structural characterization of cobalt recycled from cathodes of spent Li-ion batteries

M. B. J. G. Freitas · E. M. Garcia ·
V. G. Celante

Received: 5 February 2008 / Accepted: 15 October 2008 / Published online: 1 November 2008
© Springer Science+Business Media B.V. 2008

Abstract In this work, cobalt from spent Li-ion batteries of cellular phones was recycled using electrochemical techniques. The efficiency, structure and morphology of deposits were influenced by the pH solution and charge density. Maximum efficiency is obtained for pH = 5.40 for all charge densities analyzed. The presence of the cobalt hcp phase for both pH solutions (5.40 and 2.70) and charge density conditions (10.0 and 50.0 C cm⁻²) used in the electrodeposition process was detected by X-ray diffraction. The growth of the cobalt deposit is favored in the crystallographic direction [002] for pH = 5.40 and in the direction [110] for pH = 2.70 when the charge density is 10.0 C cm⁻². The [100] and [101] crystallographic directions of hcp phase were detected by X-ray diffractogram for both pH conditions when the charge density was increased to 50.0 C cm⁻². The potentiodynamic dissolution of the cobalt depends on its structural composition.

Keywords Li-ion batteries · Cobalt electrodeposition · Cobalt

1 Introduction

Li-ion batteries are used in portable devices such as cellular telephones and microcomputers since they have a

greater power density than either Ni–Cd or Ni–MH batteries [1]. In the year 2000, the world production of Li-ion batteries reached 500 million cells and will reach 4.0 billion in 2008 [2]. LiCoO₂ is the cathode material most employed in Li-ion batteries. Consequently, the residue generated by spent Li-ion batteries is composed of 5.0–15.0% cobalt. The utilization of cobalt in the Li-ion batteries has increased the bulk price from US \$15 to US \$54 per kilogram between 2003 and 2004 [3]. Therefore, it is necessary to recycle the positives electrodes. The electrochemically recovered cobalt may be used to make alloys with magnetic properties or new electrodes [4, 5]. The solution composition directly influences the cobalt electrodeposition mechanism and the deposit morphology. The formation of cobalt films can occur in two-dimensional (2D) or three-dimensional (3D) dimensions, also denominated as lateral or perpendicular growth mechanisms, respectively [6]. In electrodeposited cobalt, the phases present are the compact hexagonal (hcp) and/or face centered cubic (fcc). The formation of the cobalt fcc is promoted by the co-deposition of atomic hydrogen. However, during and after the electrodeposition, the fast diffusion of the hydrogen causes the formation of the more stable hcp phase. According to the work of Nakahara and Mahajan [7] and later Cohen-Hyans [8], in low pH (approximately 1.6), electrodeposited cobalt in sulfate solutions consists mainly of fcc, and, for pH above of 5.7, the majority structure is the hcp. Our previous work studied the pH influence in electrochemical recycling of cobalt present in the spent Li-ion batteries cathodes [9]. The objective of this work is to analyze the effect of charge density (q) and solution pH on the electrodeposition efficiency, morphology, and crystalline structure of the cobalt electrodeposits.

M. B. J. G. Freitas (✉) · E. M. Garcia · V. G. Celante
Departamento de Química, Laboratório de Eletroquímica
Aplicada, Universidade Federal do Espírito Santo,
Av. Fernando Ferrari 514, Goiabeiras, Vitória,
ES CEP: 29070-910, Brasil
e-mail: marcosbj@hotmail.com; marcosbj@gmail.com

2 Experimental

2.1 Material characterization

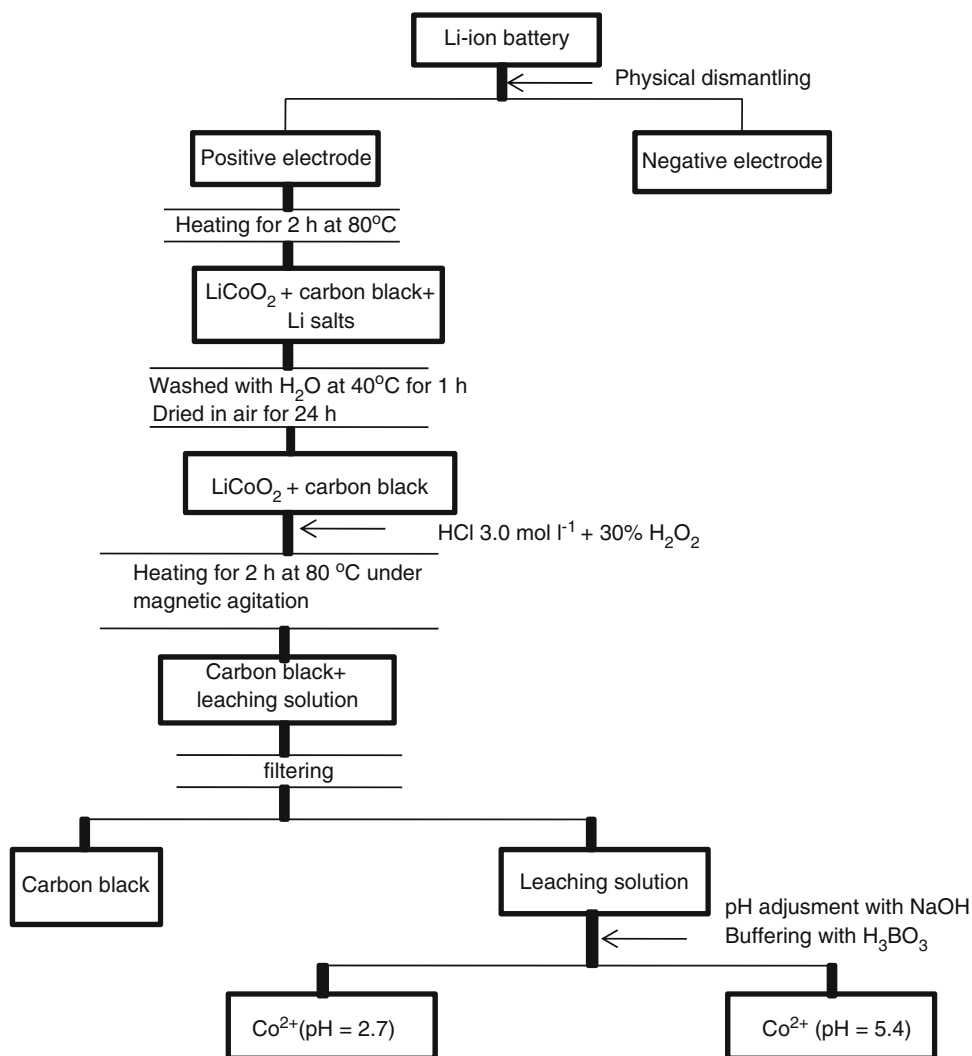
The electrodeposits were characterized with the following techniques: X-ray diffraction, scanning electronic microscopy (SEM), and energy dispersive X-ray analysis (EDX). X-ray diffraction measurements were carried out in a 200 B Rotaflex-Rigaku with copper K radiation, Ni filter, and a scan velocity of 2 min^{-1} . SEM and EDX measurements were done with a JEOL JXA model 8900 RL equipped with an energy dispersive X-ray detector. Atomic absorption spectroscopy measurements were measured with an AAS model AA-1275A from Intralab.

2.2 Preparation of electrodeposition solutions

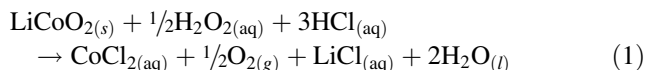
Li-ion batteries were manually dismantled and physically separated into their different parts: anode, cathode, steel,

separators, and current collectors. In the method for recycling the positives electrodes of Li-ion batteries described by Mansur and Dorella [10], the leaching is done at $60 \text{ }^\circ\text{C}$ for 2 h to evaporate organic compounds, such as ethylene carbonate (EC) and propylene carbonate (PC). For better solvent evaporation, we increased the leaching temperature to $80 \text{ }^\circ\text{C}$ for 2 h. This process also facilitates the detachment of the active material from the respective current collectors. The electrodes were washed in distilled water at $40 \text{ }^\circ\text{C}$ under agitation for 1 h to remove possible lithium salts such as LiPF_6 and LiCl_4 and dried in air for 24 h. A mass of 9.17 g of positive electrodes was dissolved in a solution containing 470.00 ml of HCl 3.00 mol L^{-1} and 30.00 mL H_2O_2 30% v/v, and the system was maintained under constant magnetic agitation at $80 \text{ }^\circ\text{C}$ for 2 h. The insoluble carbon black was separated by filtration from the leaching solution. The cathode dissolution efficiency increased with acid concentration and temperature. The addition of H_2O_2 is necessary to increase the efficiency of

Fig. 1 Flow-sheet for cobalt recycled from cathodes of spent Li-ion batteries



cathode dissolution. H_2O_2 reduces cobalt from oxidation state +III, which is insoluble in aqueous systems to +II, which is soluble in water. Considering the active material $LiCoO_2$, the cathode dissolution reaction is represented by Eq 1:



The pH of the leaching solution was adjusted with NaOH pellets to 2.7 and 5.40. The solutions were buffered with $0.10 \text{ mol L}^{-1} H_3BO_3$. The function of H_3BO_3 was to maintain constant pH of the electrodeposition bath because it influences the efficiency and morphology of electrodeposits as shown in as described in Sect. 3.3. The ionic cobalt concentration in the baths was equal to 0.10 mol L^{-1} measured by atomic absorption spectroscopy (AAS). A flowchart for cobalt recycled from cathodes of spent Li-ion batteries is given in Fig. 1.

2.3 Electrochemical measurements

Electrochemical measurements were performed with a power supply model MQPG-01 from Microchemistry. The working electrodes were 99.99% Al (MERCK) and prepared as a rectangular foil with a geometric area of 0.40 cm^2 . The auxiliary electrode was platinum and had an area of 3.75 cm^2 . The reference electrode was saturated Ag/AgCl/NaCl. The working electrodes were sanded with 600-grit sandpaper before each measurement and then washed with distilled water. Potentiostatic measurements were made applying potentials of -1.00 V . The charge densities (q) applied were 10.0 , 50.0 , and 100.0 C cm^{-2} . The charge efficiency (α) was calculated using the Faraday's law. The electrodeposits formed in potentiostatic conditions were dissolved in a $0.50 \text{ mol L}^{-1} H_2SO_4$ solution under potentiodynamic polarization. The initial equilibrium potential was -0.44 V , and the end potential was 0.60 V . The potential scan rate was 10.00 mV s^{-1} . All the electrochemical measurements were accomplished without solution agitation at $25 \text{ }^\circ\text{C}$.

3 Results and discussion

3.1 Charge efficiency

In order to analyze the efficiency of the ionic cobalt electrodeposition, different values of charge densities were applied, and the potential of -1.00 V was held constant. The charge efficiency is larger for cobalt electrodeposited from solutions with pH 5.40 for all experimental values of charge densities (Fig. 2). This occurs due to the decreased

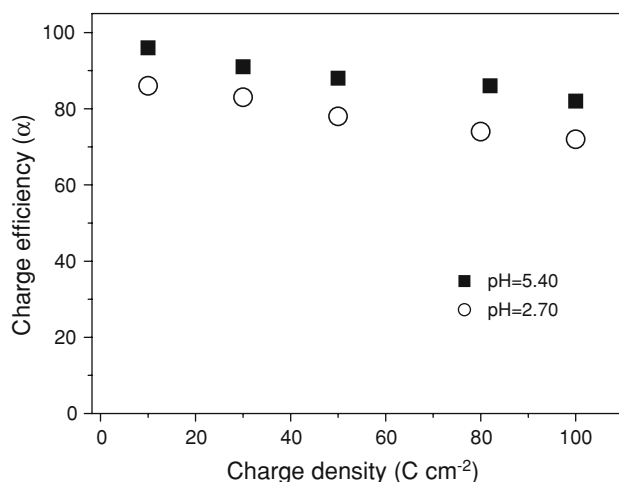


Fig. 2 Charge efficiency vs. charge density for cobalt electrodeposition for a potential of -1.00 V . The cobalt concentration was 0.10 mol L^{-1} , pH = 5.40 and 2.70 with $0.10 \text{ mol L}^{-1} H_3BO_3$ as a buffer

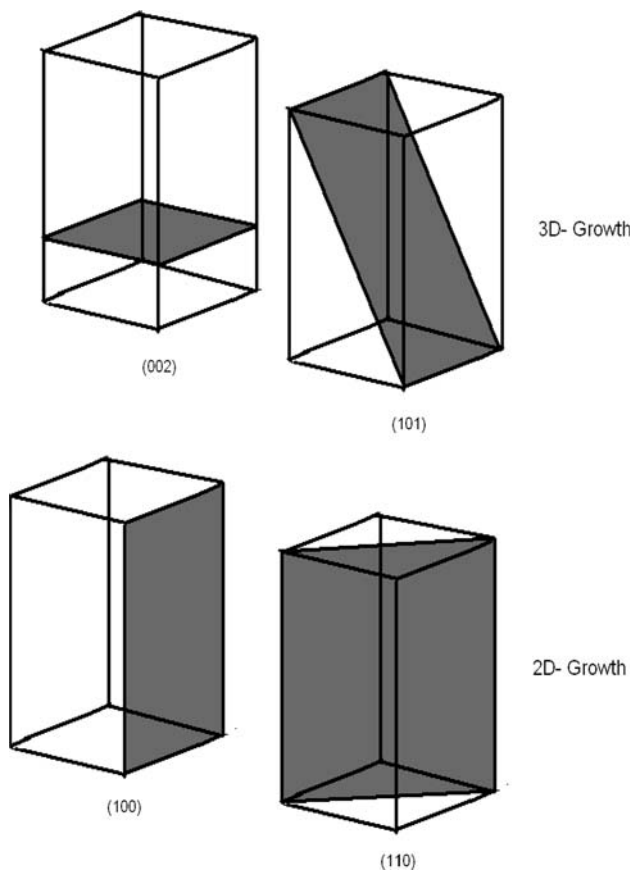
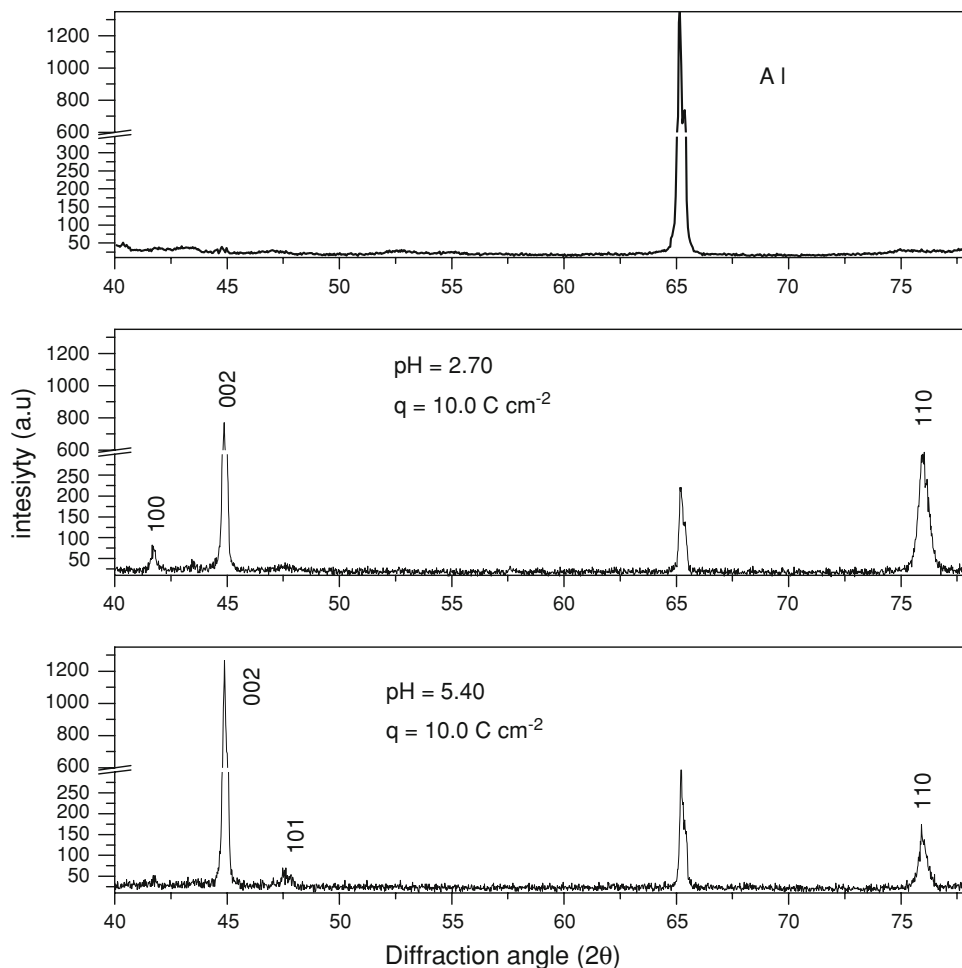


Fig. 3 Representations of the crystallographic plans for 3D and 2D growth in hexagonal compact phase (hcp)

contribution of the proton reduction reaction. The efficiency decrease occurs because the ionic cobalt concentration decreases with increasing charge density.

Fig. 4 The X-ray diffractograms for the cobalt electrodeposits obtained from a solution with cobalt concentration of 0.10 mol L^{-1} , pH = 5.40 and 2.70, $0.10 \text{ mol L}^{-1} \text{ H}_3\text{BO}_3$ as a buffer, potential of -1.00 V , and $q = 10.0 \text{ C cm}^2$



3.2 X-ray diffraction of cobalt electrodeposits

The cobalt structure is strongly influenced by nucleation and growth processes [11–13]. Figure 3 shows the crystallographic preferential directions attributed to the perpendicular (3D) and lateral (2D) growth. The growth of the crystallographic plan depends on the electrodeposition conditions. The influence of pH and charge density on the crystalline structure of cobalt was studied by performing the electrodeposition at a potential of -1.00 V under different pH conditions. A typical X-ray diffractogram of cobalt electrodeposited under an Al substrate with charge density of 10.0 C cm^{-2} in different pH solutions is given in Fig. 4. In comparison with the Joint Committee on Powder Diffraction Standards (JCPDS) [14], the peaks [002] and [110] of the cobalt hcp phase are observed for both pH solutions. However, small differences are verified in the X-ray diffractogram when the peaks intensities are analyzed. Growth in the [002] direction of cobalt electrodeposits is more intense for pH = 5.40. The [110] direction is favored for pH = 2.70. Thus, it is possible to detect that

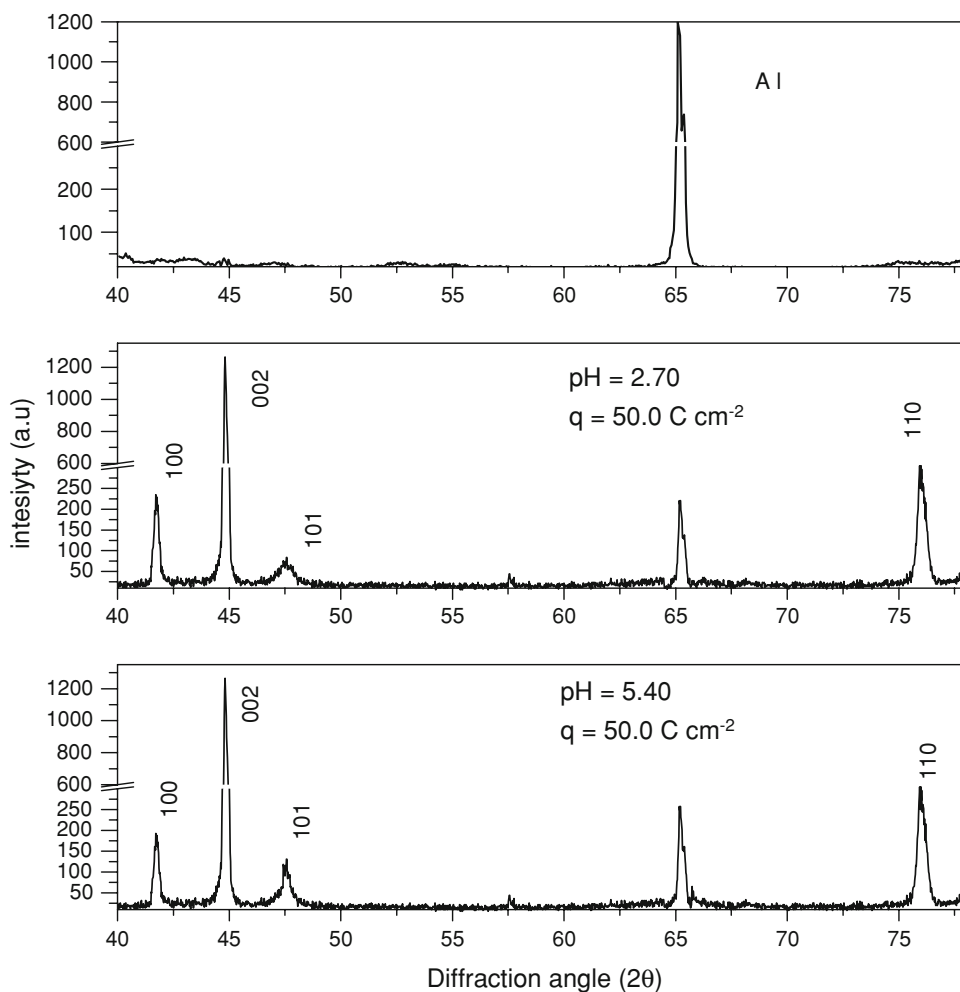
3D growth is preferred at pH = 5.40 and that 2D growth is preferred at pH = 2.70. Matsushima [15] also observed this behavior.

Figure 5 shows typical X-ray diffractograms of cobalt electrodeposits under Al substrate with a charge density of 50.0 C cm^{-2} and the solution pH of either 5.40 or 2.70. The peaks in the [002] and [001] directions have the same intensities. Using X-ray diffraction, it is possible to observe the [100] and [101] peaks for cobalt electrodeposited from different pH conditions. The peak intensity in [100] direction has 2D growth characteristics and is observed for cobalt electrodeposited at pH = 5.4; the [101] peak was characteristic of 3D growth and observed for cobalt deposited at pH = 2.7. These confirm the hybrid 2D and 3D models proposed for cobalt deposit growth.

3.3 SEM and EDX of cobalt electrodeposits

Experiments were done to understand the impact of charge density and pH solution on the morphology of cobalt

Fig. 5 The X-ray diffractograms for the cobalt electrodeposits obtained from a solution with cobalt concentration of 0.10 mol L^{-1} , pH = 5.40 and 2.70, $0.10 \text{ mol L}^{-1} \text{ H}_3\text{BO}_3$ as a buffer, potential of -1.00 V , and $q = 10.0$ and 50.0 C cm^{-2}



electrodeposits. Figures 6 and 7 show the SEM image of cobalt electrodeposited at pH = 5.40 and 2.70, respectively. The cobalt electrodeposited at a solution pH of 5.4 is present as large macrospores (Fig. 6). This suggests that macroporosity is larger with increases in charge density. This is in agreement with the previous observation that the perpendicular growth or 3D mechanism is favored at pH = 5.4. This preferential growth mechanism for cobalt morphology results in macrospores. For cobalt electrodeposited at a solution pH of 2.7, the 2D mechanism is favored. The deposit surface is more regular, and macroporosity is reduced, as can be seen in Fig. 7. Matsushima [15] and Gómez [16] also observed this behavior. As has been noted in previous work [9], for pH = 2.70 the initial stage of formation of cobalt electrodeposits is instantaneous nucleation. This favors the formation of a great quantity of short nuclei. Deposit formation at pH = 5.40 tends towards progressive nucleation with the formation of large nuclei in small quantity.

Figure 8 shows an energy dispersive X-ray analysis for cobalt electrodeposits where only cobalt was detected.

3.4 Potentiodynamic dissolution of cobalt electrodeposits

The electrodeposits formed at -1.00 V and charge densities of 10.00 C cm^{-2} and 50.0 C cm^{-2} were dissolved in a $0.50 \text{ mol L}^{-1} \text{ H}_2\text{SO}_4$ solution by the potentiodynamic technique (Fig. 9). Only one dissolution peak is observed in Fig. 9a. As noted in Sect. 3.2, the [002] and [110] peaks are more intense when the charge density for cobalt electrodeposition is equal to 10.0 C cm^{-2} . X-ray diffraction measurements can be used to assign the dissolution peaks to these planes. The increase in the charge density to 50.0 C cm^{-2} is visible as one peak and a shoulder in the voltammetric dissolution for both pH conditions (Fig. 9b). The shoulder can be attributed to the dissolution of the cobalt crystallographic directions [100] and [101].

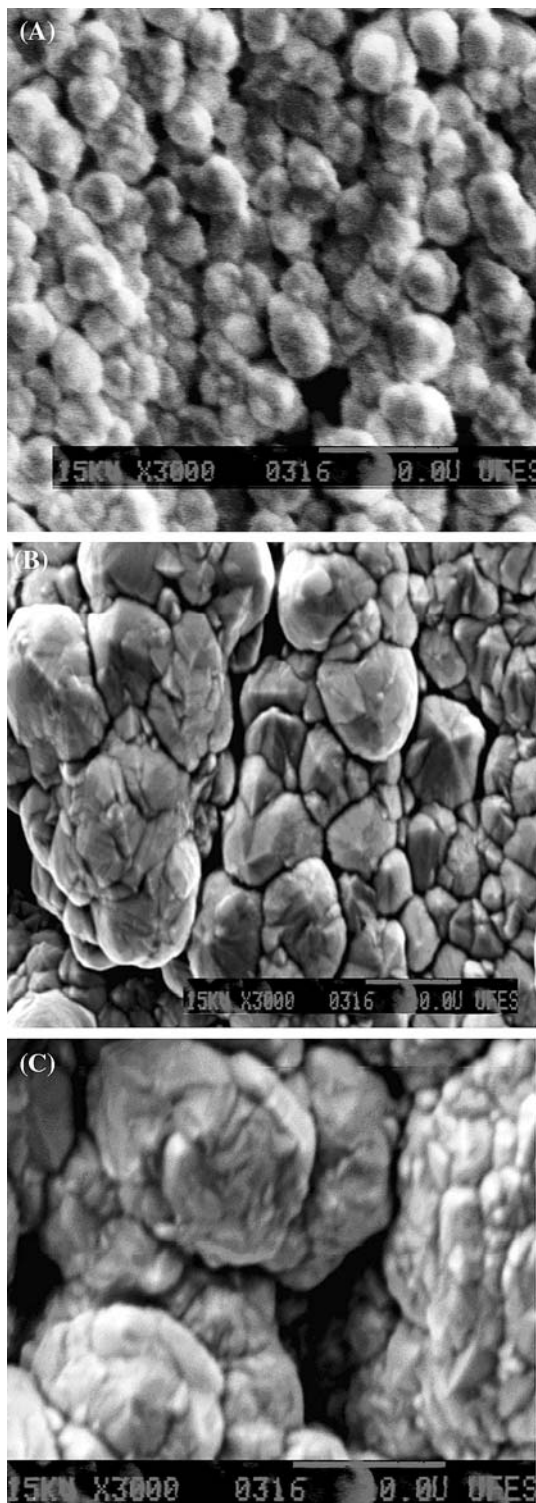


Fig. 6 The scanning electron microscopy (SEM) for cobalt electro-deposits obtained from a solution with a cobalt concentration of 0.10 mol L^{-1} , $\text{pH} = 5.40$ with $0.10 \text{ mol L}^{-1} \text{H}_3\text{BO}_3$ as a buffer. The charge density (q) utilized was equal to: **a** 10.0, **b** 50.0 and **c** 100.0 C cm^{-2} and a potential of -1.00 V

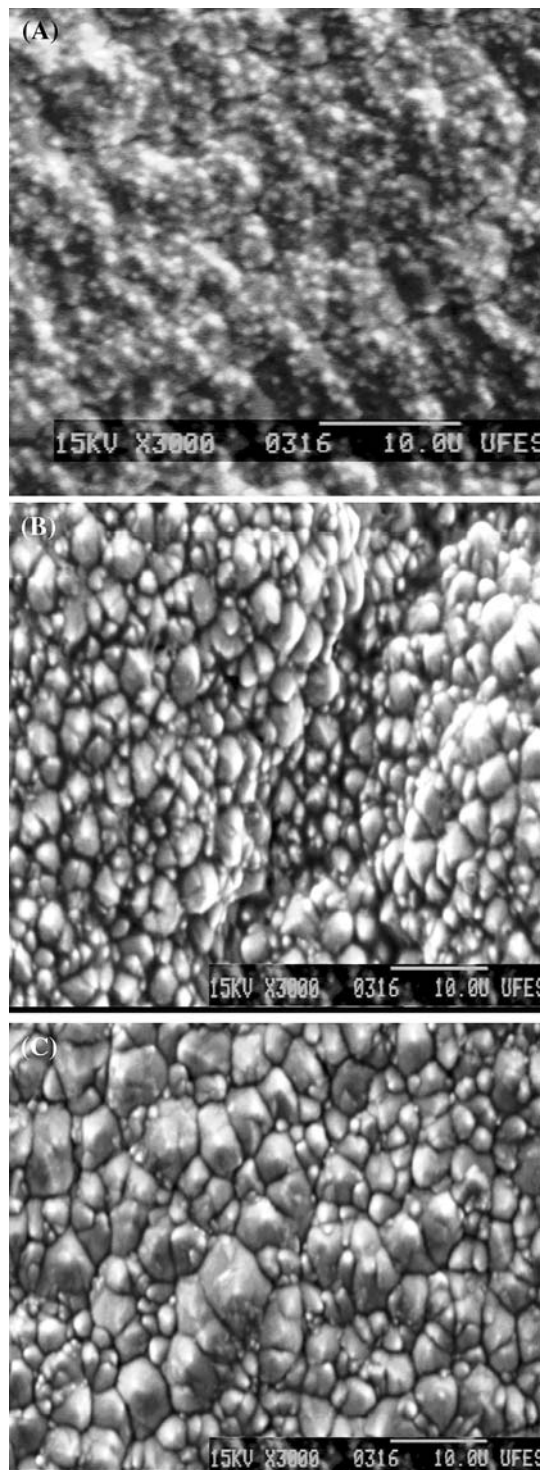


Fig. 7 The scanning electron microscopy (SEM) for cobalt electro-deposits obtained from a solution with a cobalt concentration of 0.10 mol L^{-1} , $\text{pH} = 2.70$ with $0.10 \text{ mol L}^{-1} \text{H}_3\text{BO}_3$ as a buffer. The charge density (q) utilized was equal to: **a** 10.0, **b** 50.0 and **c** 100.0 C cm^{-2} and a potential of -1.00 V

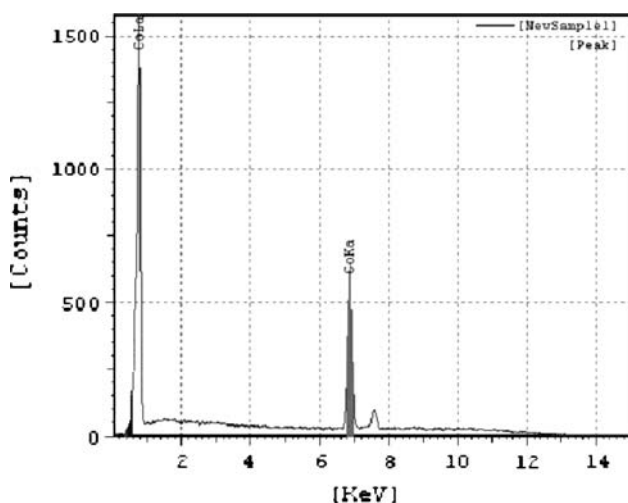


Fig. 8 The typical energy dispersive of X-ray (EDX) for cobalt electrodeposits obtained from a solution with cobalt concentration of 0.10 mol L^{-1} , $\text{pH} = 5.40$ with H_3BO_3 0.10 mol L^{-1} as buffer

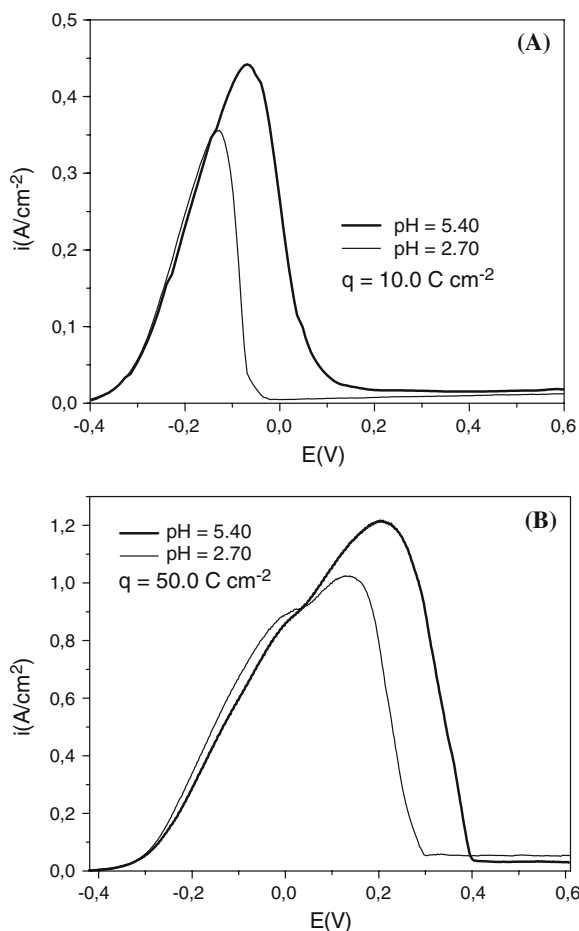


Fig. 9 Voltammetric curves for dissolution of cobalt electrodeposited with potential same to -1.00 V and charge density of 10.0 C cm^{-2} (a) and 50.0 C cm^{-2} (b) in the H_2SO_4 solution ($\text{pH} = 0.5 \text{ mol L}^{-1}$) with a scan rate of 10.0 mV s^{-1}

4 Conclusion

The charge efficiency is greater for cobalt electrodeposition carried out in $\text{pH} = 5.40$ compared to $\text{pH} = 2.70$ for all values of charge density. The reduction of hydrogen ions lessens with increasing solution pH. Growth in the [002] direction is favored for $\text{pH} = 5.40$ and in the [110] direction for $\text{pH} = 2.70$. It was observed that 3D growth is favored at $\text{pH} = 5.40$ and that 2D growth is favored at $\text{pH} = 2.70$ at a charge density of 10.0 C cm^2 . The effects of increasing charge density on the crystallographic directions [100] and [101] for the hcp phase are shown in a X-ray diffractogram at both pH conditions. In the potentiodynamic dissolution, the shoulder preceding the anodic peak indicates to the [100] and [101] directions.

Acknowledgement The authors acknowledge MCT-CNPq-FAPES process 36303542/2007 for its financial support.

References

1. Takeno K, Ichimura M, Takano K et al (2005) *J Power Sources* 142:298
2. Cobalt Development Institute (2005) In: Cobalt News Available in: <http://www.thecdi.com> Cited 14 Apr 2007
3. Jandova J, Vu H, Dvorak P (2005) *Hydrometallurgy* 77:67
4. Krause A, Hamann C, Uhlemann M et al (2005) *J Magn Magn Mater* 290:261
5. Jyoko Y, Kashiwabara S, Hayashi Y (1997) *J Electrochem Soc* 144:5
6. Schmid M, Lundgren E, Leonardelli G et al (2001) *J Appl Phys* 72:405
7. Nakahara S, Mahajan S (1980) *J Electrochem Soc* 127:283
8. Cohen-Hyans Kaplan WD, Yahalom J (2002) *Electrochem Solid-State Lett* 5:C75
9. Freitas MJB, Garcia EM (2007) *J Power Sources* 171:953
10. Mansur MB, Dorella G (2007) *J Power Sources* 170:210
11. Jiang SP, Chen YZ, You JK et al (1990) *J Electrochem Soc* 137:3374
12. Gunawardena G, Hills G, Montenegro I et al (1982) *J Electroanal Chem* 138:225
13. Scharifker B, Hills G (1983) *Electrochimica Acta* 28:879
14. Joint Committee on Powder Diffraction Standards (JCPDS), Card No. JCPDS 05-0727
15. Matsushima H, Ispas A, Bund A et al (2007) *J Solid-State Electrochem* 11:737
16. Gómez E, Vallés E (2002) *J Appl Electrochem* 32:693